Available online at www.sciencedirect.com

ScienceDirect

Procedia CIRP

www.elsevier.com/locate/procedia

7th HPC 2016 – CIRP Conference on High Performance Cutting

Robust stability of machining operations in case of uncertain frequency response functions

David Hajdu[a,*], Tamas Insperger[a], Gabor Stepan[a]

[a]*Budapest University of Technology and Economics, Budapest, Hungary*

* Corresponding author. *E-mail address:* hajdu@mm.bme.hu

Abstract

Prediction of machine tool chatter requires a dynamic characterization of the machine-tool-workpiece system by means of frequency response functions (FRFs). Stability lobe diagrams are sensitive to the uncertainties of the measured FRF, which reduces the reliability of their industrial application. In this paper, a frequency-domain method is presented to determine robust stability boundaries with respect to the uncertainties of the FRF. The method is based on an envelope fitting around the measured FRFs combined with some considerations of the single-frequency method. The application of the method is validated on a turning operation characterized by a series of FRF measurements. It is shown that stability analysis using the averaged FRF may considerably overestimate the region of robust stability.

Peer-review under responsibility of the International Scientific Committee of 7th HPC 2016 in the person of the Conference Chair Prof. Matthias Putz.

Keywords: Turning; chatter; uncertainty; frf; robustness

1. Introduction

Reliable prediction of machining parameters without producing machine tool chatter is a highly important task for machine tool centers. One of the most accepted explanation for machine tool chatter is the surface regeneration: the vibrations of the tool are copied onto the surface of the workpiece, which modifies the chip thickness and induces variation in the cutting force one revolution later [1], [2]. From dynamic systems point of view, chatter is associated with the loss of stability of the steady-state (chatter-free) machining process followed by a large amplitude self-excited vibration between the tool and the workpiece usually involving intermittent loss of contact. Stability properties of machining processes are depicted by the so-called stability lobe diagrams, which plot the maximum stable depths of cut versus the spindle speed. These diagrams provide a guide to the machinist to select the optimal technological parameters in order to achieve maximum material removal rate without chatter.

Stability lobe diagrams can be calculated using frequency domain techniques, such as the single frequency solution, the multi-frequency solution [3] [4], and the extended multi-frequency solution [5]. These methods apply the measured frequency response functions (FRFs) directly. In contrast, time-domain solutions, such as the semi-discretization method [6], full-discretization method [7], spectral element method [8] or the implicit subspace iteration method [9], just to mention a few, require fitted modal parameters as input. In spite of the available efficient numerical techniques, experimental cutting tests do not always match the predicted stability lobe diagrams [10]. One reason for these differences is the uncertainties of the measured FRFs. For frequency-domain methods, these uncertainties directly affect the generated stability lobe diagrams. For time-domain methods, the uncertainties of the FRF are manifested as uncertainties of the fitted modal parameters, which, again, affect stability lobe diagrams. In this latter case, the number of modes to be involved in the fitting and the properties of the mechanical model used for the fitting (e.g., proportional vs. non-proportional damping, symmetric vs. non-symmetric FRF matrix) also strongly affect the structure of the stability lobe diagrams [5], [11]. These cases demonstrate

Peer-review under responsibility of the International Scientific Committee of 7th HPC 2016 in the person of the Conference Chair Prof. Matthias Putz.

that robustness of the generated stability lobe diagrams is an important issue for practical applications.

A robust method called Edge Theorem combined with Zero Exclusion condition is presented in [12], [13], which can be applied for low number of uncertain parameters. The algorithm, however, leads to intensive numerical computation with many limitations, hence the „robust formulation cannot accommodate more than two varying parameters due to increasing model complexity" [13].

In this paper, a frequency-domain technique is presented for the calculation of the robust stability boundaries in case of uncertain FRFs. The method is based on an envelope fitting around the measured FRF combined with the concept of the single frequency solution, which essentially reduces the computational effort.

2. Mechanical model of turning operations

The dynamical model of an orthogonal cutting operation with multiple vibration modes is shown in Fig. 1. The modes are projected to direction *z*, which is the direction of the surface regeneration. A multiple-degree-of-freedom model is considered with *n* number of modes and with the generalized coordinates $\mathbf{z}(t) = (z_1(t), z_2(t) \dots z_n(t))^{\mathrm{T}}$. The cutting force acting on the tool tip assuming a nonlinear characteristics can be given as

$$F_z(t) = K_z w h^q(t), \tag{1}$$

where K_z is the cutting-force coefficient in direction *z*, *w* is the depth of cut, $h(t)$ is the instantaneous chip thickness and *q* is the cutting-force exponent. The chip thickness is affected by the current tool position and the previous position of the tool one revolution before. The regenerative time delay is $\tau = 60/\Omega$, where Ω is the workpiece revolution given in rpm. The instantaneous chip thickness then can be calculated as

$$h(t) = v_{\mathrm{f}}\tau + z_1(t-\tau) - z_1(t), \tag{2}$$

where v_{f} is the feed velocity and $z_1(t)$ indicates the position of the tool tip in direction *z*. The linearized forcing vector $\mathbf{f}(t)$ is

$$\mathbf{f}(t) = \begin{pmatrix} K_z w q (v_{\mathrm{f}}\tau)^{q-1} \big(z_1(t-\tau) - z_1(t)\big) \\ 0 \\ \vdots \\ 0 \end{pmatrix}. \tag{3}$$

3. The single-frequency method

In order to obtain a frequency-domain estimation of the robust stability boundaries, the main steps of the single-frequency method is summarized for the stability analysis of the systems with fixed FRF [14]. The definition of the FRF matrix $\mathbf{H}(\omega)$ gives

$$\mathbf{H}(\omega)\mathbf{F}(\omega) = \mathbf{Z}(\omega), \tag{4}$$

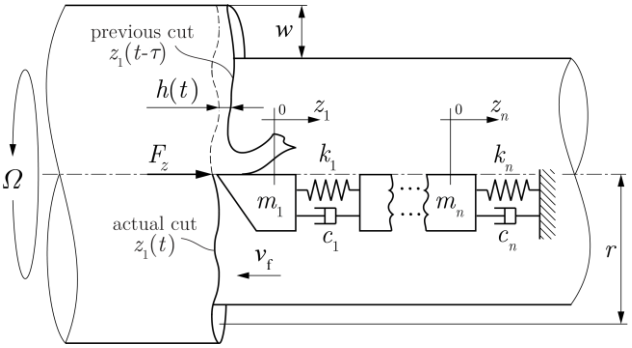

Fig. 1. Surface regeneration in turning process with multiple vibration modes.

where $\mathbf{F}(\omega)$ and $\mathbf{Z}(\omega)$ are the Fourier transforms of the forcing vector $\mathbf{f}(t)$ and displacement vector $\mathbf{z}(t)$, respectively. The Fourier transform of the linearized parametric forcing $\mathbf{f}(t)$ is given as

$$\mathbf{F}(\omega) = \boldsymbol{\kappa}(\mathrm{e}^{-\mathrm{i}\omega\tau} - 1)\mathbf{Z}(\omega), \tag{5}$$

where

$$\boldsymbol{\kappa} = \begin{pmatrix} \kappa & 0 & \cdots & 0 \\ 0 & 0 & \cdots & 0 \\ \vdots & \vdots & \ddots & \vdots \\ 0 & 0 & \cdots & 0 \end{pmatrix} \quad \text{and} \quad \kappa = K_z w q (v_{\mathrm{f}}\tau)^{q-1} \tag{6}$$

is the specific cutting-force coefficient. Substitution of Eq. (4) into Eq. (5), and simplification yield

$$\big(\mathbf{I} - (\mathrm{e}^{-\mathrm{i}\omega\tau} - 1)\boldsymbol{\kappa}\mathbf{H}(\omega)\big)\mathbf{F}(\omega) = \mathbf{0}, \tag{7}$$

where $\mathbf{I}$ is the identity matrix. The existence of the nontrivial solution implies

$$\det\big(\mathbf{I} - (\mathrm{e}^{-\mathrm{i}\omega\tau} - 1)\boldsymbol{\kappa}\mathbf{H}(\omega)\big) = 0, \tag{8}$$

which, considering the structure of $\boldsymbol{\kappa}$, can be expressed as

$$D(\omega) = 1 - (\mathrm{e}^{-\mathrm{i}\omega\tau} - 1)\,\kappa H(\omega) = 0. \tag{9}$$

Here, $H(\omega) := H_{11}(\omega)$ is the measured tip-to-tip FRF. If the inverse FRF is written as $H(\omega) = \Lambda_{\mathrm{Re}}(\omega) + \mathrm{i}\Lambda_{\mathrm{Im}}(\omega)$, then the analytic solution for the stability lobe diagrams, where Eq. (9) is satisfied, can be given as [4]

$$\Omega = \frac{30\omega}{\arctan\left(\dfrac{\Lambda_{\mathrm{Re}}(\omega)}{\Lambda_{\mathrm{Im}}(\omega)}\right) + j\pi} \quad \text{and} \quad \kappa = -\frac{\Lambda_{\mathrm{Re}}(\omega)^2 + \Lambda_{\mathrm{Im}}(\omega)^2}{2\Lambda_{\mathrm{Re}}(\omega)^2}, \tag{10}$$

where $j = 1,2,\dots,\infty$ and $\omega \in [0,\infty)$. These parametric curves gives the stability lobes in the parameter plane (Ω,κ).

4. Robust stability analysis

The FRFs obtained from measurements are always loaded by noise and uncertainties, which can be represented as an uncertain envelope around the averaged FRF. In this paper it

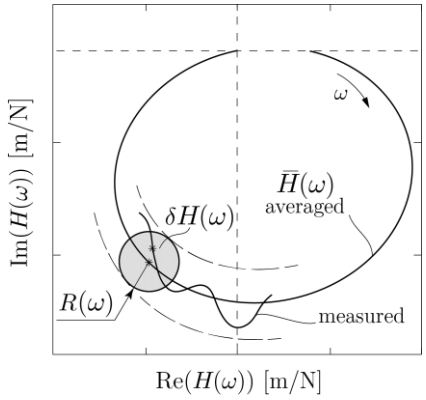

Fig. 2. Uncertainties in the frequency response function. $\bar{H}(\omega)$ is the average FRF and $\delta H(\omega)$ is the perturbation around $\bar{H}(\omega)$ with radius $R(\omega)$.

is assumed that the uncertainty can be given as an additive complex perturbation as

$$H(\omega) = \bar{H}(\omega) + \delta H(\omega), \tag{11}$$

where $\bar{H}(\omega)$ is the averaged FRF and $\delta H(\omega)$ is the perturbation around it. It is assumed that $|\delta H(\omega)| \le R(\omega)$ where $R(\omega)$ is the radius of the complex perturbation (see Fig. 2). Substitution of Eq. (11) into the characteristic equation (9) and separation to real and imaginary parts give

$$\delta H_{\mathrm{Re}}(\omega) = -\frac{1}{2\kappa} - \bar{H}_{\mathrm{Re}}(\omega), \tag{12}$$

$$\delta H_{\mathrm{Im}}(\omega) = -\frac{\sin(\omega\tau)}{2\kappa(1-\cos(\omega\tau))} - \bar{H}_{\mathrm{Im}}(\omega). \tag{13}$$

If there is a perturbation $\delta H(\omega) = \delta H_{\mathrm{Re}}(\omega) + \mathrm{i}\delta H_{\mathrm{Im}}(\omega)$, which satisfies Eqs. (12)-(13) for some ω, then the system is not robustly stable. If Eqs. (12)-(13) cannot be satisfied by the possible/allowed perturbations for any ω, then the system is robustly stable or robustly unstable depending on whether the averaged system is stable or unstable.

A bound for the uncertainties of the FRF can be given by an envelope about the averaged FRF. A possible envelope can be a tube obtained by centering discs of radius $R(\omega)$ at $\bar{H}(\omega)$ (see Fig. 2). In this case, a safety factor can be defined as

$$SF := \min_{\omega\in[0,\infty)} \frac{|\delta H_{\mathrm{Re}}(\omega) + \mathrm{i}\delta H_{\mathrm{Im}}(\omega)|}{R(\omega)}, \tag{14}$$

where $\delta H_{\mathrm{Re}}(\omega)$ and $\delta H_{\mathrm{Im}}(\omega)$ are calculated according to Eqs. (12) and (13), respectively. If $SF < 1$ then the system is not robustly stable, i.e., there exists a perturbation $|\delta H(\omega)| < R(\omega)$, for which the system is unstable. If $SF > 1$ then the system is robustly stable if the averaged model is stable or robustly unstable if the averaged model is unstable. The robust stability boundary is given by the contour curves $SF = 1$. Note that the envelope can be constructed in other ways, for instance based on the standard deviation of the measured FRFs.

5. Case study

In practical applications, the uncertainties are filtered by averaging the measured FRFs. Typically, five to ten measurements are performed and their average is used for the stability calculation [10].

In this case study, the FRF of the tip of a turning tool was measured fifty times, which provided fifty different (uncertain) FRFs due to imperfect excitation and due to noise. The individual FRFs are shown in Fig. 3 by dark gray lines, while their average is indicated by thick black line. The envelope of uncertainty radius $R(\omega)$ about the average is shown by light gray shading. This envelope compasses all the measured FRFs. It can be seen that the uncertainty envelope is considerable, especially around the first natural frequency (around 650~750Hz).

Figure 4 presents the case when the FRFs were averaged after every fifth measurement. Ten different FRFs are shown by dark gray lines, each being an average of five individual measurements. In this case the uncertainty envelope is narrower, which reflects the filtering effect of averaging the FRFs. The uncertainty around 700Hz is still remarkable.

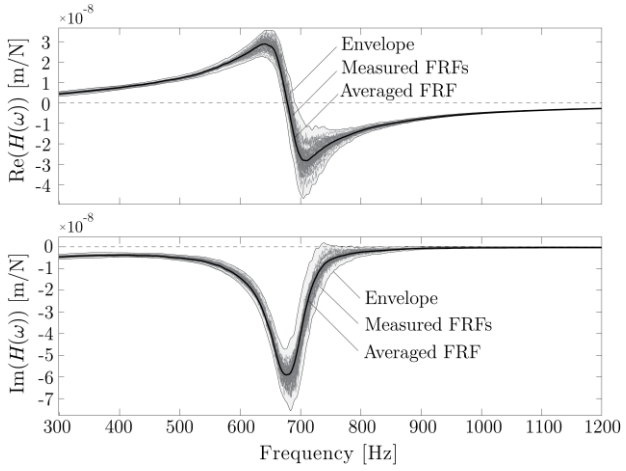

Fig. 3. Measured FRFs (solid dark gray lines), averaged FRF (solid black line) and uncertainty envelope (light gray shaded area).

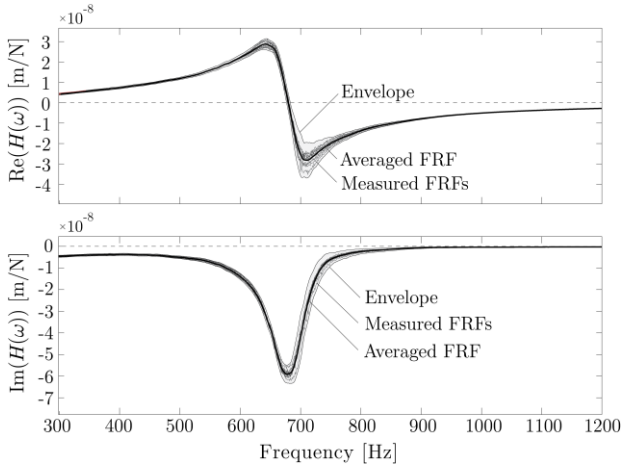

Fig. 4. Measured FRFs as an average of five measurements (solid gray lines), averaged FRF (solid black line) and uncertainty envelope (gray shaded area).

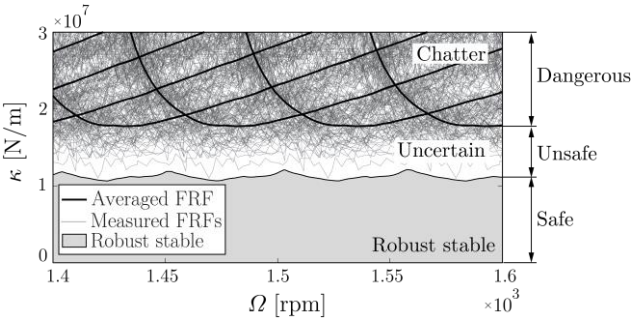

Fig. 5. Stability lobes corresponding to the individual FRFs (dark gray lines), to the averaged FRF (solid black line) and the robust stable domain obtained by the proposed method (light gray shaded area).

The stability boundaries corresponding to the fifty individually measured FRFs are presented in Fig. 5 by dark gray lines. The stability lobes associated with the averaged FRF is shown by thick black line. Light gray shaded area represents the region of robust stability determined according to the method presented in Sec. 4. It can be seen that the boundary of robust stability (SF=1) is located at lower specific cutting-force coefficient values (κ) than that of the averaged FRF. Still, the lobe-like structure of the two boundaries is similar. The region between the robust and the averaged stability boundaries is the uncertain region: stable machining operation cannot be guaranteed in this region.

Figure 6 presents the robust and the averaged stability boundaries associated with the fifty FRF measurements (without averaging) for low (left) and for higher (right) spindle speeds. It can be seen that about 40% of the stable region predicted by the averaged model is actually uncertain.

Figure 7 presents the stability charts for the case when the FRFs were averaged after every fifth measurements. The uncertainty region is still significant, it occupies about 20~25% of the stable region predicted by the averaged model.

6. Conclusion

Prediction of the stability of machining operations always involves several uncertainties. Dynamic behavior of the machine-tool-workpiece system is a typical uncertain component, which is usually overcome by averaging a series of FRFs. In this paper, a frequency-domain method was presented to calculate the robust stability analysis of turning operations using directly the measured FRFs. The method is based on an envelope fitting around the measured FRFs combined with some considerations of the single-frequency method.

Application of the method to a series of FRF measurements of a turning tool showed that the robust stability boundaries can significantly be smaller than the stability boundaries corresponding to the averaged FRF. The analysis demonstrated that the actual robust stability boundary can well be approximated by the proposed method. It was also demonstrated that using the average of five FRF measurements still overestimates the region of robust stability. This observation may explain the disagreement between stability lobe predictions and actual cutting tests, which is often experienced in machine tool chatter research.

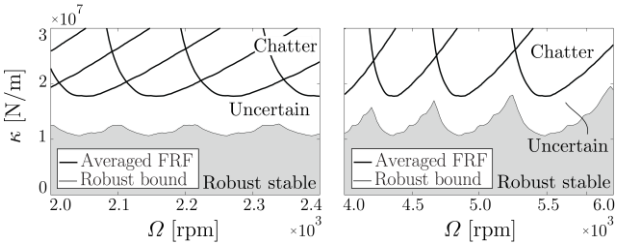

Fig. 6. Stability lobe diagrams at different spindle speeds obtained from fifty FRFs (no averaging during the measurement).

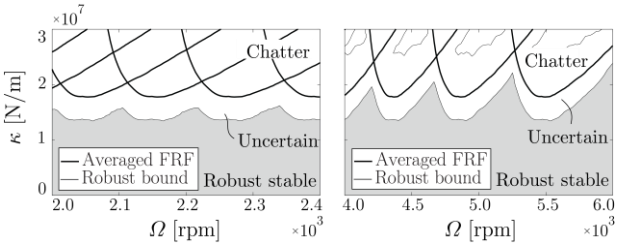

Fig. 7. Stability lobe diagram at different spindle speeds obtained from ten FRFs, each being an average of five individual measurements.

Acknowledgements

This work was supported by the Hungarian National Science Foundation under grant OTKA-K105433. The research leading to these results has received funding from the European Research Council under the European Unions Seventh Framework Programme (FP/2007-2013) / ERC Advanced Grant Agreement n. 340889.

References

[1] Tobias S, Machine-tool Vibration. Glasgow, Blackie; 1965.
[2] Tlusty J, Spacek L. Self-excited vibrations on machine tools (in Czech.), Prague: Nakl. CSAV; 1954.
[3] Altintas Y, Budak E. Analytical prediction of stability lobes in milling. CIRP Ann–Manuf Techn 1995; 44:357-362.
[4] Altintas Y, Budak E. Analytical prediction of chatter stability in milling, Part I: General formulation. J Dyn Syst–T ASME 1998; 120:22-30.
[5] Bachrathy D, Stepan G. Improved prediction of stability lobes with extended multi frequency solution. CIRP Ann–Manuf Technol 2013; 62:411-414.
[6] Insperger T, Stepan G. Semi-discretization for time-delay systems. New York: Springer; 2011.
[7] Ding Y, Zhu LM, Zhang XJ, Ding H, A full-discretization method for prediction of milling stability. Int J Mach Tool Manu 2010; 50-502-509.
[8] Khasawneh FA, Mann BP. A spectral element approach for the stability of delay systems. Int J Numer Meth Eng 2011; 87:566-952.
[9] Zatarian M., Dombovari Z. Stability analysis of milling with irregular pitch tools by the implicit subspace iteration method. Int J Dynam Control 2014; 2:26-34.
[10] Stepan G, Munoa J, Insperger T, Surico M, Bachrathy D, Dombovari Z. Cylindrical milling tools: comparative real case study for process stability. CIRP Ann–Manuf Techn 2014; 63(1):385-388.
[11] Munoa J., Dombovari Z., Mancisidor I., Yang Y., Zatarain M. Interaction between multiple modes in milling processes. Mach Sci Technol 2013; 17:165-180.
[12] Park S. S., Qin Y. M. Robust regenerative chatter stability in machine tools. Int J Adv Manuf Technol 2007; 33:389–402.
[13] Graham E., Mehrpouya M., Park S.: Robust prediction of chatter stability in milling based on the analytical chatter stability. Journal of Manufacturing Processes 2013; 15:508-517.
[14] Altintas Y. Manufacturing Automation - Metal Cutting Mechanics, Machine Tool Vibrations and CNC Design. 2nd ed. Cambridge: Cambridge University Press; 2012.